Journal of Electroceramics 4:2/3, 427–432, 2000
© 2000 Kluwer Academic Publishers. Manufactured in The Netherlands.

Magnetoresistance in Tunnel Junctions Made of Epitaxially Grown Manganate Films with 1.6-nm-Thick Barriers

TAKESHI OBATA,* TAKASHI MANAKO, YUICHI SHIMAKAWA & YOSHIMI KUBO

Fundamental Research Laboratories, NEC Corporation, 34 Miyukigaoka, Tsukuba, Ibaraki 305-8501, Japan

Abstract. Magnetic tunnel junctions with barrier thicknesses of either 1.6 or 2.4 nm have been fabricated from epitaxially grown $La_{0.8}Sr_{0.2}MnO_3/SrTiO_3/La_{0.8}Sr_{0.2}MnO_3$ trilayers. For the junctions with 1.6-nm-thick $SrTiO_3$, tunneling magnetoresistance (TMR) as large as 150% was observed at 5 K. A small TMR was observed even at 270 K, which is close to the ferromagnetic Curie temperature (290 K) of the $La_{0.8}Sr_{0.2}MnO_3$ film. Besides tunneling conduction, parallel semiconduction through the $SrTiO_3$ barrier appeared to exist, and became dominant at high temperatures, reducing the TMR ratio and operating temperature, especially for thicker $SrTiO_3$ barriers. The $SrTiO_3$ barrier thickness is the key to improving TMR characteristics, and fabricating a sufficiently thin and uniform barrier layer is essential for achieving a large TMR and a high operating temperature.

Keywords: manganate, tunneling magnetoresistance, tunnel junction

1. Introduction

Large magnetoresistance in a low magnetic field (less than a few hundreds oersted) has been observed recently in spin-dependent tunneling through grain boundaries and heteroepitaxial junctions with perovskite-type hole-doped manganates, such as $La_{1-x}Sr_xMnO_3$ [1–6]. This large tunneling magnetoresistance (TMR) can be attributed to the nearly 100% spin polarization of conduction electrons in the manganates, where only a single-spin band crosses the Fermi level [7–9]. Considering a magnetic tunnel junction (ferromagnetic electrode/insulating barrier/ferromagnetic electrode), the TMR ratio is given by [10]

$$\Delta R_j(H)/R_j(H) = 2P_1P_2/(1 - P_1P_2) \qquad (1)$$

where $R_j(H)$ is the junction resistance in the field of H, $\Delta R_j(H) = R_j(0) - R_j(H)$, and P_1 and P_2 are the spin polarizations of the two ferromagnetic electrodes. Hence, junctions using the manganates have a great advantage over those using typical ferromagnetic metals and alloys, of which the spin polarizations are in the range of 0.2–0.4 [11]. By using the high degree of spin polarization available from the manganates, we can make magnetoelectronic devices, such as highly sensitive magnetic sensors or magnetic random access memories.

In most of the results reported so far, however, TMR in magnetic tunnel junctions disappeared at temperatures far lower than the Curie temperatures (T_C) of the manganates. For junctions of *in situ* grown $La_{1-x}Sr_xMnO_3/SrTiO_3/La_{1-x}Sr_xMnO_3$ ($x = 0.3$ or 0.33) trilayers [3–5], maximum operating temperatures (T_{op}) are around 200 K, which are far lower than T_Cs of the manganate films (350 K for $x = 0.3$ and 370 K for $x = 0.33$). In these junctions, the thickness of STO barriers (t_b) were from 3 to 6 nm, which were much larger than those of Al_2O_3 barriers (1–2 nm) used in junctions with typical ferromagnetic metals and alloys [12]. Although ramp-edge junctions with thin STO barriers ($t_b = 2$ nm) showed a higher T_{op} equal to 0.8 of T_C [6], these junctions exhibited small TMR ratios ($\leq 23\%$) even at low temperatures. These low TMR ratios might be caused by degradation of the interfaces between the manganates and barriers due to the *ex situ* deposition.

*E-mail: obata@frl.cl.nec.co.jp

Such low operating temperatures as well as low TMR ratios are obstacles to their applications at room temperature. From these reported results, the thickness of the barrier and the quality of the interface appear to be the keys to improving TMR characteristics in junctions with manganates. In this study, we have fabricated magnetic tunnel junctions comprising *in situ* and epitaxially grown $La_{0.8}Sr_{0.2}MnO_3/SrTiO_3/La_{0.8}Sr_{0.2}MnO_3$ (LSMO/STO/LSMO) trilayers with different STO barrier thicknesses, and we experimentally confirmed the effect of the barrier thickness on the TMR characteristics. The TMR characteristics of the junctions with sufficiently thin STO barriers $(t_b = 1.6\,\text{nm})$ are significantly improved, and we have observed a TMR ratio as large as 150% at 5 K under a low magnetic field (<10 Oe). We have also observed a small TMR even at 270 K, which reaches 0.92 of the T_C of the LSMO film.

2. Experimental

The LSMO/STO/LSMO trilayer was grown by pulse laser deposition (PLD) *in situ* to keep the interfaces free from contamination. The bottom LSMO layer was grown on a polished $SrTiO_3$ (1 0 0) single crystal at 650–700°C under the oxygen pressure of 300 mTorr [13,14]. The T_C of the LSMO layer, determined by magnetization and resistivity measurements (Fig. 1), was 290 K, which was slightly lower than that reported for LSMO single crystals (≈ 310 K) [15]. The resistivity at 5 K(600–700 $\mu\Omega$cm) was as small as that for single crystals. The coercive force (H_c) in the plane was less than 10 Oe, suggesting high quality of the crystallinity. The STO barrier layer was grown on the bottom LSMO at 600°C under 50 mTorr of oxygen, and then the top LSMO layer was grown under the same conditions as the bottom LSMO layer was. Finally, the trilayer was cooled to room temperature under 760 Torr of oxygen. The top and bottom LSMO layers were 50 nm thick, and the STO barrier layer was either 1.6 or 2.4 nm thick. High-resolution transmission electron microscopy (HRTEM) revealed that each layer was epitaxially grown as shown in Fig. 2. Even for $t_b = 1.6$ nm, the STO barrier layer was uniformly grown between the top and bottom LSMO layers, and the interfaces were atomically sharp and flat.

Micron-scale junctions (Fig. 3) were fabricated from the trilayer by conventional photolithography [14]. The trilayer was patterned to form a large bottom electrode by using ion milling through a photoresist stencil. Rectangular junctions with areas (S_j) of $2\times30, 5\times30$, and $10\times50\,\mu$m were then defined by using another photoresist stencil and ion milling etching timed to end at the top surface of the bottom LSMO electrode. Such rectangular shapes were adopted in order to make the coercivity larger by the shape-anisotropic demagnetization field effect. Then the junctions were coated with a 100-nm-thick SiO_2 insulation layer by vacuum evaporation. The stencil was subsequently lifted off to open self-aligned contact windows. The top LSMO and STO layers were removed from the contact windows on the bottom LSMO electrodes to achieve a low base

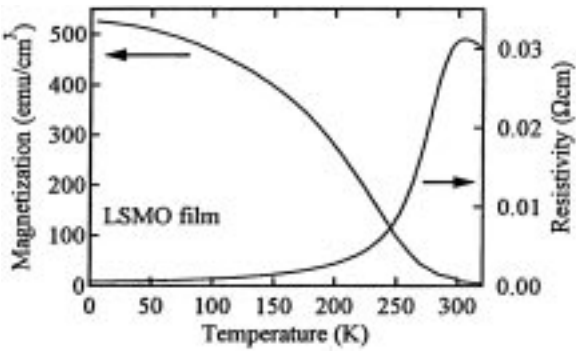

Fig. 1. Temperature dependence of the spontaneous magnetization and the resistivity for an LSMO film.

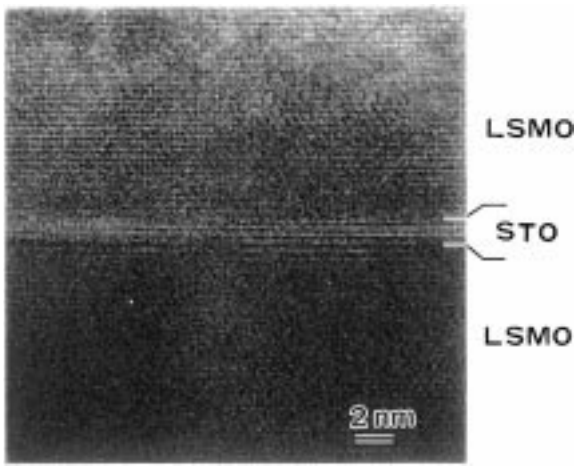

Fig. 2. Cross-sectional lattice image of the interface within an LSMO/STO/LSMO trilayer by HRTEM.

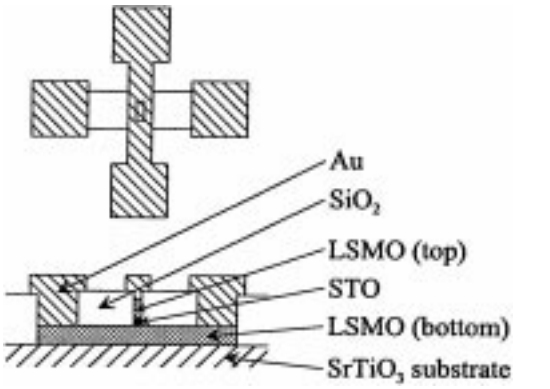

Fig. 3. A planar and a cross-sectional views of a magnetic tunnel junction using an LSMO/STO/LSMO trilayer.

resistance. Finally a gold layer was deposited and patterned to form contact electrodes.

Junction properties were investigated by measuring dc conductance and magnetoresistance in the temperature range from 4.2 to 300 K using the conventional 4-terminal method.

3. Results and Discussion

The inset of Fig. 4(a) shows the change in R_j against the applied magnetic field at 5 K for a junction with $S_j = 5 \times 30\,\mu$m and $t_b = 1.6$ nm. The magnetic field was applied along the longitudinal direction of the top LSMO layer. The magnetic moments of the top and bottom LSMO layers were aligned in parallel for high magnetic fields, and low R_j was observed. In contrast, when the magnetic moments were aligned in antiparallel for low fields due to the difference in the coercivities of the two LSMO layers, a high R_j was observed. Since R_j was constant above 1000 Oe, the TMR ratio in the field of H was defined by $[R_j(H) - R_j(1500\,\text{Oe})]/R_j(1500\,\text{Oe})$. The main panel of Fig. 4(a) shows a magnified view of the inset. The TMR ratio changed sharply below 25 Oe. Coercivities for the bottom and top LSMO layers were estimated to be a few Oe and 15–25 Oe, respectively. The former value is consistent with the H_c observed for the individual LSMO film, while the latter larger coercivity is due to the shape-anisotropic demagnetization field effect. A TMR ratio as large as 150% was observed in the junction. The spin polarization P of the LSMO layers estimated from Eq. (1) was 0.65.

Although this P is considerably higher than those for typical ferromagnetic metals and alloys, it is lower than unity. Also, the peaks of the TMR hysteresis curve slightly differ in height and location. This ''low'' P value and the asymmetry of the TMR hysteresis curve suggest incomplete antiparallel alignment of the magnetic moments of both LSMO layers. For the top LSMO layer, since the coercivity was due to the shape-anisotropic demagnetization effect, it was probable that orientations of magnetic domains were not uniform, especially near the edge of the rectangular. To achieve the complete antiparallel alignment of the magnetic moments, a magnetically biasing layer, such as an antiferromagnetic layer,

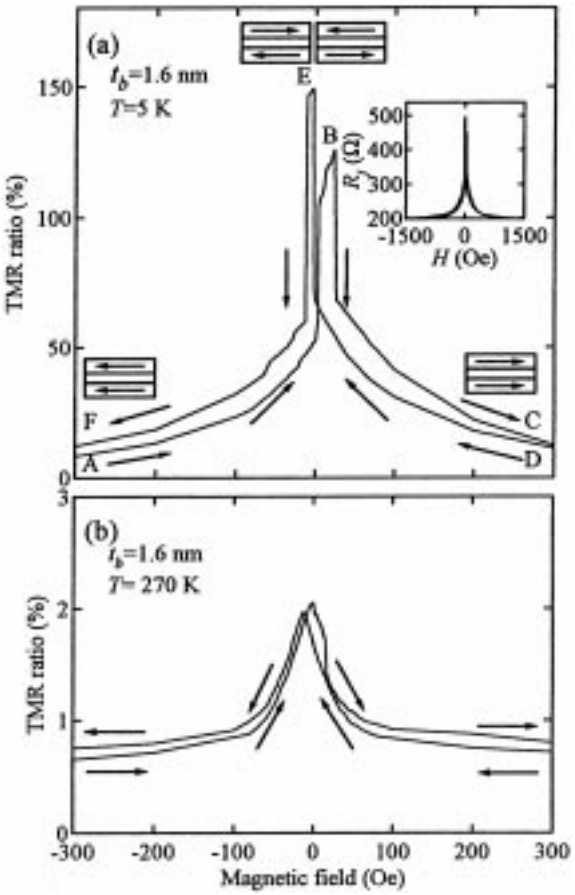

Fig. 4. Change in the TMR ratio against the applied magnetic field in a junction ($S_j = 5 \times 30\,\mu$m and $t_b = 1.6$ nm) at (a) 5 K and (b) 270 K. The inset of (a) shows the change in the junction resistance over a wider range of applied magnetic fields. The arrows show the direction of the sweeping magnetic field. The orientation of the magnetic moments of two LSMO layers is also shown in (a).

should be deposited on the top (or the bottom) LSMO layer to pin the magnetic moment, and thus enable larger TMR ratio.

Figure 4(b) shows the magnetoresistance at 270 K for the same junction as in Fig. 4(a). TMR (2%) was observed even at 270 K. The observed TMR was not caused by the colossal magnetoresistance (CMR) effect of the LSMO film. Since the CMR ratio of the individual LSMO film in low magnetic fields was small ($\leq 0.2\%$) at this temperature, the observed TMR ratio of 2% was the result of spin-dependent tunneling through the junction. T_{op} of 270 K was very close to the T_C (290 K) of the individual LSMO film, and the T_{op} normalized to the T_C was 0.92. These results clearly demonstrate that both a large TMR ratio and a high operating temperature can be achieved in junctions made with perovskite manganates.

Next, we will consider the effect of STO barrier thickness on TMR. Figure 5 shows the temperature dependence of the TMR ratios for various junctions with $t_b = 1.6$ and 2.4 nm. The junctions with $t_b = 1.6$ nm showed higher TMR ratios than those with $t_b = 2.4$ nm at the same temperature. In addition, the TMR ratios for the junctions with $t_b = 2.4$ nm decayed faster than those for the junctions with $t_b = 1.6$ nm. A similar fast decay of the TMR ratio with increasing temperature has been reported, where thicker STO barriers (3–6 nm) were fabricated [3,4,5]. Although the existence of a magnetically dead layer at the surface of the LSMO film at high temperatures has been suggested to explain the previous results [16], our results demonstrate that spin-dependent tunneling is observable even at temperatures close to T_C if sufficiently thin STO barriers are successfully fabricated.

Figure 6 shows the temperature dependence of the area-scaled junction resistances $R_{jp} \times S_j$ measured under the parallel magnetic moment orientation of the two LSMO layers for various STO-barrier thicknesses. For the present junctions, since $R_{jp} \times S_j$ was independent of S_j for the same t_b, the observed R_{jp} represents the intrinsic nature of the junction [14]. The value of $R_{jp} \times S_j$ for $t_b = 2.4$ nm were, as expected, higher than those for $t_b = 1.6$ nm in the measured temperature range, but the temperature dependence for both thickness showed an unusual feature. $R_{jp} \times S_j$ first gradually increased with increasing temperatures, reaching a maximum at a characteristic temperature T_{Rmax}, then decreased. A similar behavior was observed for the junctions with thick STO barriers ($t_b = 3$–6 nm) by Sun et al. [17] as shown in Fig. 6. Such a feature can be qualitatively explained in terms of parallel conduction through tunneling and semiconducting paths. The gradual increase in $R_{jp} \times S_j$ up to T_{Rmax} is mainly due to the decrease in a spin polarization P, which is thought to be proportional to the spontaneous magnetization M_s of the LSMO layers, with increasing temperature, because the junction conductance of the spin-dependent tunneling $G_p = 1/R_{jp}$ is proportional to $(1 + P^2)/2$ [10].

On the other hand, the parallel semiconduction will dominate the transport of the junctions above T_{Rmax}, which will reduce $R_{jp} \times S_j$. Thus, T_{Rmax} represents a

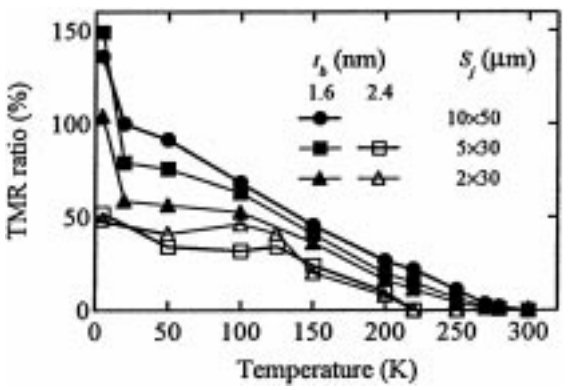

Fig. 5. Temperature dependence of the maximum TMR ratios in the parallel magnetic moment orientation of two LSMO layers for junctions with various S_j and t_b.

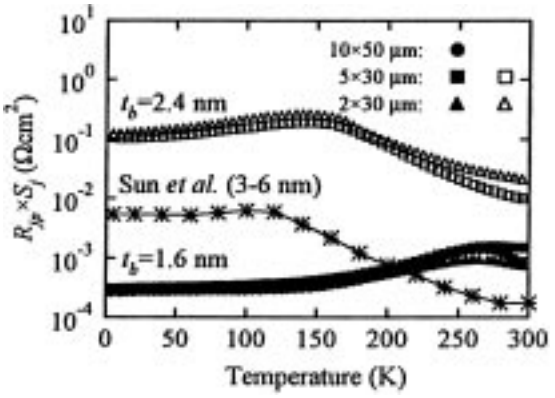

Fig. 6. Temperature dependence of the area-scaled junction resistance $R_{jp} \times S_j$ for junctions with various S_j and t_b. Previously reported data by Sun et al. [17] for thick STO barriers (3–6 nm) are drawn for comparison.

crossover temperature where the main conduction process changes from tunneling to the semiconduction. As t_b increases, the resistance of the tunneling increases exponentially, while the semiconducting resistance increases linearly. As a result, T_{Rmax} falls with increasing t_b as shown in Fig. 6. Although the data for thick STO barriers ($t_b = 3$–$6\,\mathrm{nm}$) showed lower $R_{jp} \times S_j$ than those for the present junctions with $t_b = 2.4\,\mathrm{nm}$ (this may be due to the difference in junction quality), it showed a similar tendency of the lower T_{Rmax} for the larger t_b. We stress that TMR always disappears just above T_{Rmax}. This is consistent with the dominance of the semiconduction, which strongly reduces the TMR ratio, above T_{Rmax}. Therefore, fabricating a sufficiently thin barrier is essential to achieve a high operating temperature.

To estimate the average barrier height ϕ and the barrier thickness s from the current-voltage characteristics, we corrected the observed G_p with the spin-polarization P. Figure 7 shows the applied voltage dependence of the corrected tunneling conductance G_c at various temperatures for a junction with $t_b = 1.6\,\mathrm{nm}$ and $S_j = 2 \times 30\,\mu\mathrm{m}$, written as,

$$G_c = G_p / \left(\frac{1 + P^2}{2} \right) \tag{2}$$

$$= \alpha(1 + 3\gamma V^2) \tag{3}$$

where α and γ are functions of ϕ and s [10,18]. The results of the fitting to Eq. (3) are also plotted in Fig. 7. (Here, we used the normalized magnetization $M_s(T)/M_s(T = 5\,\mathrm{K})$ instead of P.) The conductance curves observed at high temperatures are well reproduced by Eq. (3). From the fitting, we obtained estimated barrier thicknesses s of 2.3 to 2.4 nm and average barrier heights ϕ of 0.24 to 0.27 eV in the temperature range of 150 to 250 K. For the junction with a designed barrier thickness t_b of 2.4 nm, a similar fitting gave s of 3.2 to 3.3 nm and ϕ of 0.27 to 0.29 eV below 150 K. The estimated barrier thicknesses were slightly larger than the designed thicknesses. The differences in the thickness (0.7–0.9 nm), however, correspond to the two unit cells of LSMO. Thus, this result indicates that only one unit cell of each top and bottom LSMO acts as an insulating barrier at the LSMO/STO interfaces. The estimated barrier heights (0.24–0.29 eV) are comparable to those reported so far [5,17], though they are lower than those expected from the band gap of STO ($\sim 3.0\,\mathrm{eV}$). Such a low barrier height may be

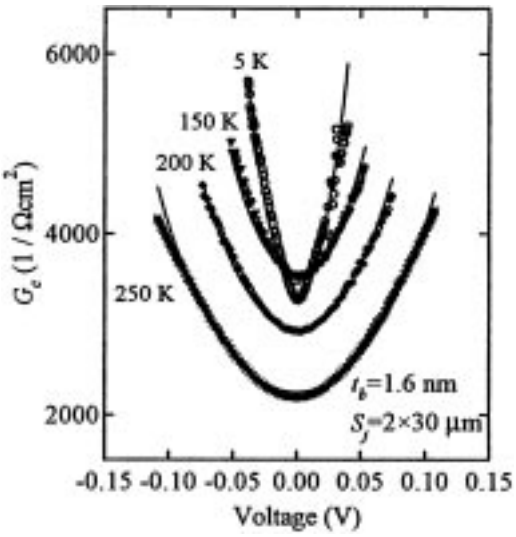

Fig. 7. Corrected dc conductance G_c vs applied voltage in a magnetic junction ($S_j = 2 \times 30\,\mu\mathrm{m}$ and $t_b = 1.6\,\mathrm{nm}$) at 1500 Oe under various temperatures. The solid lines show the results of the fitting to Eq. (3).

explained in terms of the electron doping of the STO. It is well known that the electron doping caused by an oxygen deficiency [19] or cation substitution [20] leads to semiconduction or even metallic conduction in STO. An oxygen deficiency and/or substitution of Sr^{2+} in the STO with La^{3+} at the LSMO/STO interfaces are possible origins for the electron doping because of the rather low oxygen pressure and high substrate temperature during the deposition of the LSMO/STO/LSMO trilayers. The electron doping of the STO can also account for the parallel semiconduction that dominated the transport of the junctions at high temperatures.

Although tunneling appeared to dominate the transport of the junctions, the observed conductance curve at low temperatures cannot be fitted to Eq. (3) completely because of a small zero-bias anomaly. Such zero-bias anomalies are often observed in magnetic tunnel junctions. Magnon [21] or metal inclusion [22], which have been discussed to explain this anomaly, may have occurred in the present junctions.

4. Summary

We fabricated magnetic tunnel junctions by using epitaxially grown LSMO/STO/LSMO trilayers with

different STO barrier thicknesses. With the 1.6-nm-thick STO barrier layer, a large TMR ratio of 150% was observed in the junction. Spin-dependent tunneling dominated the conduction process up to temperatures very close to the Curie temperature of the LSMO film (290 K), and a small TMR of 2% was observed at 270 K. The observed current-voltage curves were well reproduced by a modified expression of tunnel conduction with correction for the spin-polarization. The estimated average barrier height was 0.24 to 0.27 eV and the barrier thickness was 2.3 to 2.4 nm, which is slightly larger than the designed thickness. For the junctions with 2.4-nm-thick STO barriers, on the other hand, the parallel semiconduction seemed to be dominant at high temperatures, which reduced both the TMR ratio and the operating temperature. These results show that fabricating sufficiently thin STO barrier layers is the key to increasing the TMR ratio and the operating temperature. These findings are a step towards applying magnetic tunnel junctions made with spin-polarized manganates to magnetoelectronic devices.

Acknowledgments

We thank Tsutomu Yoshitake and Tetsuo Satoh for their useful discussions concerning junction fabrication. We are also grateful for the support of Toshinari Ichihashi in the HRTEM observations.

References

1. H.Y. Hwang, S-W. Cheong, N.P. Ong, and B. Batlogg, *Phys. Rev. Lett.*, **77**, 2041 (1996).
2. N.D. Mathur, G. Burnell, S.P. Isaac, T.J. Jackson, B.-S. Teo, J.L. MacManus-Driscoll, L.F. Cohen, J.E. Evetts, and M.G. Blamire, *Nature*, **387**, 266 (1997).
3. J.Z. Sun, W.J. Gallagher, P.R. Duncombe, L. Krusin-Elbaum, R.A. Altman, A. Gupta, Y. Lu, G.Q. Gong, and G. Xiao, *Appl. Phys. Lett.*, **69**, 3266 (1996).
4. Y. Lu, X.W. Li, G.Q. Gong, G. Xiao, A. Gupta, P. Lecoeur, J.Z. Sun, Y.Y. Wang, and V.P. Dravid, *Phys. Rev. B.*, **54**, R8357 (1996); J.Z. Sun, L. Krusin-Elbaum, P.R. Duncombe, A. Gupta, and R.B. Laibowitz, *Appl. Phys. Lett.*, **70**, 1769 (1997).
5. M. Viert, M. Drouet, J. Nassar, J.P. Contour, C. Fermon, and A. Fert, *Europhys. Lett.*, **39**, 545 (1997).
6. C. Kwon, Q.X. Jia, Y. Fan, M.F. Hundley, D.W. Reagor, J.Y. Coulter, and D.E. Peterson, *Appl. Phys. Lett.*, **72**, 486 (1998).
7. Y. Okimoto, T. Katsufuji, T. Ishikawa, A. Urushibara, T. Arima, and Y. Tokura, *Phys. Rev. Lett.*, **75**, 109 (1995).
8. J.-H. Park, E. Vescovo, H.-J. Kim, C. Kwon, R. Ramesh, and T. Venkatesan, *Nature*, **392**, 794 (1998).
9. W.E. Pickett and D.J. Singh, *Phys. Rev. B.*, **53**, 1146 (1996).
10. M. Julliere, *Phys. Lett.*, **54A**, 225 (1975).
11. P.M. Tedrow and R. Meservey, *Phys. Rev. B.*, **7**, 318 (1973); R. Meservey, D. Paraskevopoulos, and P.M. Tedrow, *Phys. Rev. Lett.*, **37**, 858 (1976).
12. J.S. Moodera, E.F. Gallagher, K. Robinson, and J. Nowak, *Appl. Phys. Lett.*, **70**, 3050 (1997).
13. T. Manako, T. Obata, Y. Shimakawa, and Y. Kubo, in *Science and Technology of Magnetic Oxides Symposium* edited by M. Hundley, J. Nickel, R. Ramesh, and Y. Tokura (Material Research Society, Warrendale, (1998), p. 15.
14. T. Obata, T. Manako, Y. Shimakawa, and Y. Kubo, *Appl. Phys. Lett.*, **74**, 290 (1999).
15. Y. Tokura, A. Urushibara, Y. Moritomo, T. Arima, A. Asamitsu, G. Kido, and N. Furukawa, *J. Phys. Soc. Jpn.*, **63**, 3931 (1994).
16. J.-H. Park, E. Vescovo, H.-J. Kim, C. Kwon, R. Ramesh, and T. Venkatesan, *Phys. Rev. Lett.*, **81**, 1953 (1998).
17. J.Z. Sun, L. Krusin-Elbaum, P.R. Duncombe, A. Gupta, and R.B. Laibowitz, *Appl. Phys. Lett.*, **70**, 1769 (1997).
18. J.G. Simmons, *J. Appl. Phys.*, **35**, 2655 (1964).
19. H. Yamada and G.R. Miller, *J. Solid State Chem.*, **6**, 169 (1973).
20. H.P.R. Frederiske, W.R. Thurber, and W.R. Hosler, *Phys. Rev.*, **134**, A442 (1964).
21. S. Zhang and P.M. Levy, *Phys. Rev. Lett.*, **79**, 3744 (1997).
22. J.Z. Sun, D.W. Abraham, K. Roche, and S.S.P. Parkin, *Appl. Phys. Lett.*, **73**, 1008 (1998).